

Quantum State Tomography as a Bilevel Problem

Georgios Korpas and Jakub Marecek

Department of Computer Science, Czech Technical University in Prague, Karlovo nam. 13, Prague 2, Czech Republic

It is natural to ask how to utilize actual measurements, such as the so-called IQ-plane data obtained in the dispersive readout of transmon qubits, in the estimation of the state of a quantum system. We formulate the joint problem of discrimination and quantum state tomography as a bilevel optimization problem and show how to solve it. The use of the joint problem can improve the sample complexity (or the reconstruction error for a fixed number of measurements) compared with traditional techniques that decompose the problem into the discrimination and state tomography based on the estimated expectation values of certain projective measurement operators.

1 Introduction and motivation

The development and validation of small but non-trivial quantum devices have already had a significant impact, e.g. [1, 2, 3, 4]. However, further progress is required to validate, benchmark, and fully exploit such quantum devices. In general, quantum system identification refers to the collections of techniques and protocols employed for this purpose [5]. At the most basic, one wishes to reconstruct a state's density matrix from the measurement of an ensemble of copies of a quantum state, associated with a quantum device of interest, which is known [5, 6] as quantum state tomography (QST). A QST schematic is presented in Fig. 1.

QST can be performed using many classical techniques, such as maximum likelihood estimation, compressed sensing, and Bayesian state tomography, among others. The development of such techniques is a subject of intense research, for example, in the context of matrix product states, [7], using neural networks [8], optimizing

Georgios Korpas: georgios.korpas@fel.cvut.cz
Jakub Marecek: jakub.marecek@fel.cvut.cz

circuits for noisy gates [9], while recently a great deal of attention has been paid to the use of the classical shadow [10]. Although these techniques are well established, some issues remain. The key issue is that these techniques require heavily pre-processed data as input. To be more precise, the output measurements are often considered at a very abstract level: the empirical estimates of the expectation values of certain projective measurement operators. These can be obtained only at the end of a nontrivial measurement chain involved in the readout of the quantum devices and with a substantial amount of signal processing. For example, superconducting qubits [11, 12], and increasingly also quantum dots/spin qubits [13], tend to utilize the so-called dispersive readout, which we explain in further detail in the following, but which produces a complex-valued signal in response to a so-called readout pulse [14]. This signal is processed into the so-called IQ-plane data, which are complex valued. The empirical estimates of the expectation values are then obtained from the IQ-plane data using the so-called discrimination procedure.

In this paper, we show how to perform QST from raw data, prior to discrimination. Specifically, our main result is the problem formulation

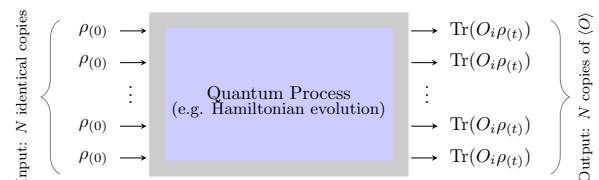


Figure 1: Several copies of a known input state $\rho(0)$ are fed into a quantum process and in each iteration a measurement of some observable O_i is performed. These outputs then are combined to form an empirical average of $\langle O_i \rangle$ out of which the output states can be reconstructed. The state reconstruction part is usually performed with heuristic techniques such as maximum likelihood estimation.

(8), which, at a high level, reads

$$\begin{aligned} & \arg \min_{b, \hat{\rho}} \left\| \sum_I \text{Tr}(\hat{\rho} \sigma_I) - b \right\|_2^2 \\ \text{subject to } & b \in \text{set of optimizers of a lower} \\ & \text{level optimization problem} \\ & \text{Tr}(\hat{\rho}) = 1 \\ & \hat{\rho} \in \mathbb{S}_+^2. \end{aligned} \tag{1}$$

where $\sigma_I \in \{\sigma_x, \sigma_y, \sigma_z\}$. That is, in (1) we minimize the empirical risk, where b is one of the optimal solutions to a lower-level minimization problem associated with the discrimination between basis states using the raw data. This can be seen as a joint problem of estimating the density matrix from the measurements and estimating the measurements from the raw data. In mathematical optimization, this is known as a bilevel optimization problem.

In contrast, processing the IQ-plane data into empirical estimates of the expectation values of projective measurement operators in a discrimination procedure, followed by a QST procedure utilizing empirical estimates of the expectation values, can be seen as a decomposition of the joint problem. Such a decomposition necessarily increases the overall sample complexity and may also introduce non-Gaussian artifacts in the data. This is the case especially when the procedures in the decomposed approach are suboptimal, as is the case with commonly used heuristics, such as the expectation-maximization (EM) algorithm in the discrimination and least-squares approaches that ignore the semidefiniteness of the density matrix within the QST utilizing the empirical estimates of the expectation values of projective measurement operators.

Note that the sample complexity of QST depends on the precise reconstruction method and the type of measurements performed. Although there are information-theoretic arguments showing [15] that certain algorithms are optimal with respect to the number of samples needed for the last step of the decomposition, assuming that the discrimination process is performed without any errors. In practice, there are errors that propagate from discrimination to quantum state tomography in a fashion that cannot be controlled in the traditional, decomposed approach. For example, when measuring the system state in superconducting devices, part of the erroneous results

can be due to qubit crosstalk effects which propagate to the readout fidelity and special care must be taken so as to tackle this [16].

The joint problem, which utilizes the raw data (such as the IQ-plane data or the dispersive readout signal directly, cf. Sec. 2), is capable of reducing noise and its propagation, essentially by filtering out samples of noise that contaminated the raw data, with the objective of minimizing the empirical risk in QST. This seems hard to do in a principled fashion without considering the use of the results of the discrimination. As we illustrate in Sec. 4, the joint problem makes it possible to obtain better estimates, given a certain number of samples, than using the decomposition approach. The lower sample complexity, in turn, translates to the computational efficiency of the reconstruction method; it is not uncommon to have weeks of postprocessing time for QST of non-trivial devices.

Progress in QST may have a considerable impact on progress in quantum computing in a more general sense. QST is the current *de facto* standard for the characterization and verification of quantum devices, including many randomized benchmarking procedures. For example, to implement quantum gates, one needs to characterize the operation of a quantum device by running a series of known inputs and reconstructing the corresponding outputs using QST, such as in the fidelity estimation of CNOT gates [17] using QST. Thus, the role of QST in quantum technologies is of fundamental importance.

2 Dispersive Readout of a Qubit

QST requires the acquisition of data from the quantum device that is investigated, which must be well isolated from sources of noise or dissipation from their coupled environment. Popular quantum devices that satisfy the above criteria are superconducting qubits such as transmon qubits [18], which have been popularized by IBM and Rigetti Computing, as well as xmon qubits used by Google [19]. A common practice is to couple the qubit(s) to a dispersive oscillator that has a resonant frequency that depends on the qubit state. By probing it with a pulse [14] and reading and analyzing the response pulse, one can reveal nontrivial information about the state.

The dispersive readout of the qubit refers to

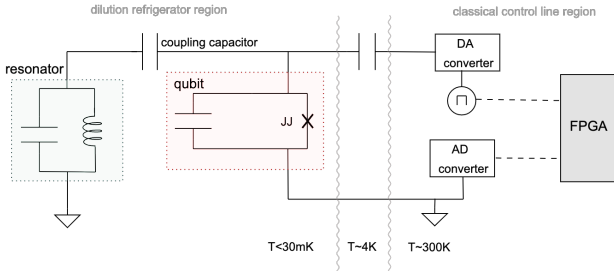


Figure 2: Simplified schematic of the transmon qubit device realized by a Josephson junction coupled to an LC resonator via a coupling capacitor. Similarly, the cavity which is kept at $T < 10\text{mK}$ (it can be lower than 3mK), is coupled to the control line via another weak coupling capacitor. The input pulse from the classical control line is converted to an analog signal, which interacts with the qubit. The output pulse passes through an AD converter to the FPGA controller interface where the I-Q readout is recorded. In this article we suggest performing QST precisely from this data, see Sec. 3 and Eq. (8).

the process of determining whether the qubit was measured in the $|0\rangle$ or the $|1\rangle$ eigenstate with respect to the measurement operator \mathbf{M} . To determine the qubit state using the readout signal as the bare minimum information on the quantum state, a number of steps are taken in the readout chain. The readout chain is made up of three levels of increasing complexity, which are commonly [20] known as:

0. *raw data* correspond to a discrete-time signal of the output pulse with frequency $\omega_{\text{r.o.}}$.
1. *IQ-plane data* corresponds to removing the frequency component of the readout signal (see Eq. 2) and obtaining the complex valued in-phase and quadrature component (IQ) data.
2. *discriminated data* which are obtained by applying a discrimination procedure to the IQ-plane data. From the discriminated data, we can obtain the so-called b -vector, cf. Eq. 3.

Only the output of the final step, i.e. the output of the discrimination procedure, is passed to QST routines.

At the raw data level, by analyzing the integrated return pulse $\omega_{\text{r.o.}}$, one can deduce whether the quantum device is in the ground state or in the excited state on the pointer basis $\{|e\rangle, |g\rangle\}$. For the purposes of this article, we can safely approximate $|g\rangle \approx |0\rangle$ and $|e\rangle \approx |1\rangle$, which correspond to the eigenstates of the observable of

the measurement apparatus, as discussed in [22]. The raw data can be mapped to the phase space (at level 1), whose precise meaning is explained below, where the output response pulse (at level 0) is represented by the amplitude response I and the phase response Q . Repetition of the measurement n times produces a mixture of two distributions in the IQ plane.

The IQ plane, which we utilize throughout this article, can be thought of as the phase space of the resonator-qubit coupled system. A comparison of the readout pulse with the original pulse using the phase shift as a result of the measurement allows one to map the qubit state onto the IQ plane. In particular, after probing the transmon qubit with a linear signal [14] of frequency ω_{probe} , one reads out the response pulse $s_{\text{r.o.}}(t) = \text{Re}(A_{\text{r.o.}} \exp(i(\omega_{\text{r.o.}}t + \vartheta)))$, where $(A_{\text{r.o.}}, \omega_{\text{r.o.}}, \vartheta)$ correspond to the amplitude, frequency, and phase of the readout pulse, respectively. At a fixed frequency $\omega_{\text{r.o.}}$, the phasor can be expressed as $s|_{\omega_{\text{r.o.}}} = \text{Re}(A \exp i\vartheta)$, which completely specifies the pulse at the given frequency. Finally, we record the *in-phase* component I and the *quadrature* component Q of the phasor:

$$\begin{aligned} s|_{\omega_{\text{r.o.}}} &= \text{Re}(A \exp i\vartheta) \\ &= I + iQ, \end{aligned} \quad (2)$$

which are known as the IQ-plane data.

In total, n repetitions of the measurement allow the computation of the empirical estimate of the expectation value of the measurement operator. On a N -dimensional measurement basis with N measurement operators, the repetition of the same procedure with further copies of the measured state (albeit possibly with different pulse frequencies) makes it possible to prepare a histogram approximation of a N -dimensional random variable, which is the input to traditional QST routines.

3 QST as bilevel SDP

Let us consider an example of the QST on a single qubit. To perform QST, one prepares an ensemble of n_I identical states ρ and performs the measurement of Pauli observables σ_I of each of these copies. Breaking away from the readout chain of the previous section, we obtain $n_I^{(0)}$ measurements corresponding to the $|0\rangle$ state and

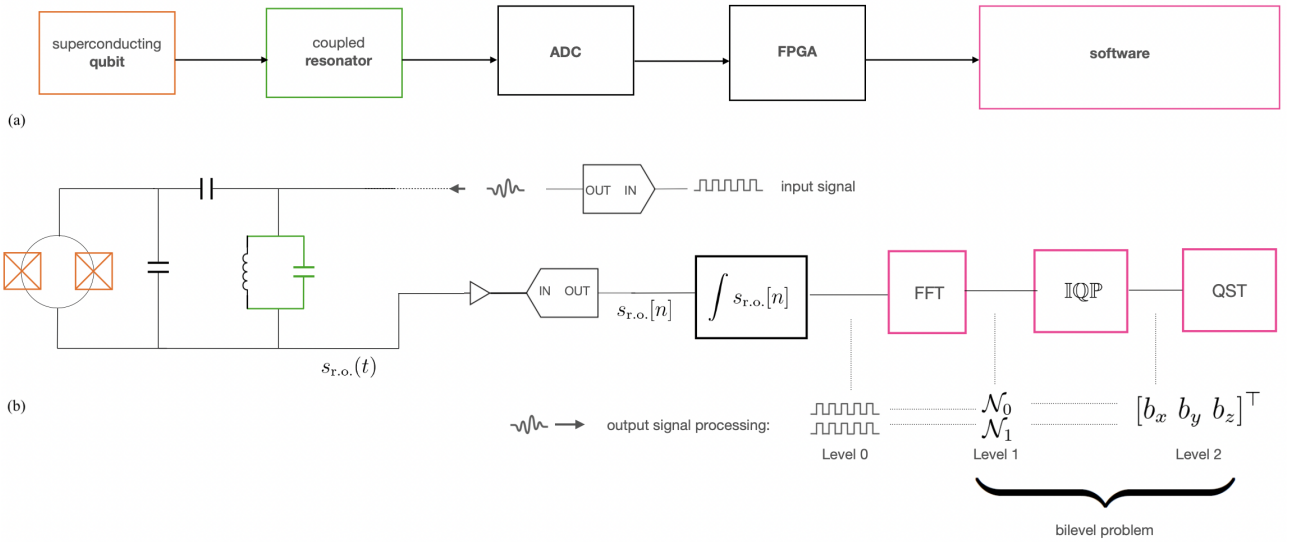


Figure 3: (a) A flow of operations in the signal readout. (b) A simplified schematic of the transmon qubit device realized by a Josephson junction coupled to an LC resonator via a coupling capacitor. See [21] for a detailed analysis of the structure. There are a number of steps in the output signal processing; our suggestion is to replace the discriminator (IQP, Eq. 11) and the traditional quantum state tomography (QST, 7) with the bilevel problem (8). See App. B for further details.

$n_I^{(1)}$ measurements corresponding to the $|1\rangle$ state where $n_I = n_I^{(0)} + n_I^{(1)}$. This corresponds to a binary vector $\beta_I \in \{0, 1\}^{n_I}$. The three measurement observables of the Pauli basis provide us with three such vectors ($\beta_x, \beta_y, \beta_z$). Out of each of these vectors, one can write the empirical estimates b_I for the expectation value of σ_I as:

$$b_I = \frac{1}{n_I} \left(\sum_{j \in n_I^{(0)}} (\beta_I)_j - \sum_{j \in n_I^{(1)}} (\beta_I)_j \right). \quad (3)$$

For a single qubit and for $n = n_x + n_y + n_z$ measurements in the Pauli basis, we obtain the following empirical estimates for the expectation values of the Pauli observables:

$$b = (b_x \ b_y \ b_z)^T \in [-1, 1]^3, \quad (4)$$

i.e., within a cube.

Traditional QST procedures use the b vector to estimate the density matrix. Thus, QST can be interpreted as a function from the polyhedron $[-1, 1]^M$ to the space \mathbb{H}_1^n of $n \times n$ Hermitian matrices with unity trace:

$$\text{QST} : [-1, 1]^M \rightarrow \mathbb{H}_1^n. \quad (5)$$

Therein, convex optimization methods provide *shape-constrained least-squares* fit. In particular, the objective of the constrained least-squares

problem is to find a unitary Hermitian matrix $\hat{\rho} \in \mathbb{H}_1^2$, which estimates the density matrix of interest, such that the ℓ_2 -norm

$$\|\mathbf{A} \text{vec}(\hat{\rho}) - b\|_2^2, \quad (6)$$

is minimized, where:

- Matrix \mathbf{A} stacks the vectorized measurement operators. For a qubit and measurement operators in the Pauli basis:

$$\mathbf{A} = [\text{vec}(\sigma_x) \ \text{vec}(\sigma_y) \ \text{vec}(\sigma_z)]^T \in \mathbb{C}^{4 \times 3},$$

- Vector b corresponds to the vector of empirical estimates of Equation (4).

Shape-constrained least squares (34) can be formulated as a semidefinite programming (SDP) problem [23]:

$$\begin{aligned} \text{QST}_{\mathbf{A}}(b) := \arg \min_{\hat{\rho} \geq 0} & \quad \|\mathbf{A} \text{vec}(\hat{\rho}) - b\|_2^2 \\ \text{subject to} & \quad \text{Tr}(\hat{\rho}) = 1. \end{aligned} \quad (7)$$

$$\hat{\rho} \in \mathbb{S}_+^2,$$

where \mathbb{S}_+^n denotes the space of positive semidefinite matrices with complex values. Solving the SDP (7) can be seen as a map from the space of recorded measurements b to the space of estimates $\hat{\rho}$, as suggested in Equation (5). Problem

(7) is easily generalized to (i) other measurement basis choices, as well as to (ii) higher-level systems with the corresponding generalization of \mathbf{A} and b .

3.1 Bilevel formulation of QST

In the preceding example and in Prob. (7), we assume that the vector b is given. Instead, we could start with the IQ-plane data and a map $\mathbb{IQP}_{\mathcal{D}_{|0\rangle,|1\rangle}}(u)_I$ from the IQ-plane data to the b -vector, which we formalize subsequently. Then, we can perform QST directly using the IQ-plane data by reformulating Prob. (7) as a bilevel problem:

$$\begin{aligned} \text{QST}_{\mathbf{A}}(b) &:= \arg \min_{b, \hat{\rho} \succeq 0} \|\mathbf{A} \text{vec}(\hat{\rho}) - b\|_2^2 \\ \text{subject to } & b_I \in [\mathbb{IQP}_{\mathcal{D}_{|0\rangle,|1\rangle}}(u)]_I \\ & \text{Tr}(\hat{\rho}) = 1 \\ & \hat{\rho} \in \mathbb{S}_+^2. \end{aligned} \quad (8)$$

where $u = \{x, y, z\}$. In the new constraint (8), b_I is defined to belong to the set of optimizers of the so-called lower-level optimization problem, which we introduce next.

Returning to the IQ-plane data, let us fix a measurement observable \mathbf{M} and let $\Omega_{\mathbf{M}} = \Omega_{\mathbf{M}}^{|0\rangle} \cup \Omega_{\mathbf{M}}^{|1\rangle}$ denote the space of possible outcomes of the measurement of the quantum device with respect to \mathbf{M} . $\Omega_{\mathbf{M}}$ is indeed the union of the outcomes that will be labeled as belonging to the $|0\rangle$ cluster, and the ones that will be labeled as belonging to the $|1\rangle$ cluster. Assuming that the recorded samples belong to a mixture of two Gaussian probability distributions $\mathcal{D}_{|0\rangle} \sim \mathcal{N}(\mu_0, \Sigma_0)$ and $\mathcal{D}_{|1\rangle} \sim \mathcal{N}(\mu_1, \Sigma_1)$, where μ_j is the mean of the j -th distribution and Σ_j is the covariance matrix of the j -th distribution, the b vector can be interpreted as the evaluation of a map ‘‘IQ-plane data $\mapsto b_I$ ’’:

$$\mathbb{IQP}_I : (\Omega_{\sigma_I}; \mathcal{D}_{|0\rangle}, \mathcal{D}_{|1\rangle}) \rightarrow [-1, 1], \quad (9)$$

the evaluation of which produces the I -th component of the b vector, the component corresponding to σ_I . Here, we index \mathbb{IQP} to stress the fact that for the full QST, one needs to perform this operation for all possible measurement operators of the measurement basis.

In the Huber contamination model, there are two distributions with parameters $\theta_0 =$

$\{\alpha_0, \mu_0, \Sigma_0\}$ corresponding to the $|0\rangle$ state, and parameters $\theta_1 = \{\alpha_1, \mu_1, \Sigma_1\}$ corresponding to the $|1\rangle$ state, and the mixing coefficient α_3 for an unknown arbitrary distribution $g(x)$ corresponding to adversary noise. Then, \mathbb{IQP} of Equation (9) corresponds to

$$f(u_s) = \sum_{i=\{1,2\}} \mathcal{D}_{|i\rangle}(u_s) + \alpha_2 g(u_s) \quad (10)$$

$$\text{where } \mathcal{D}_{|i\rangle}(u_s) := \frac{1}{\sqrt{2\pi}} \frac{\alpha_i}{|\Sigma_i|^{\frac{1}{2}}} e^{(u_s - \mu_i)^\top \Sigma_i^{-1} (u_s - \mu_i)},$$

with $\alpha_0 + \alpha_1 + \alpha_2 = 1$, $\alpha_i \in [0, 1]$, $\forall i \in \{0, 1, 2\}$, and u_s is the random variable corresponding to the sample s . We can now define \mathbb{IQP} from Equation (9) exactly as follows. First, we define:

$$f_{\mathbb{IQP}} := \sum_{s=1}^{|S_I|} \left[\sum_{i \in \{0,1\}} c_s^{(i)} \log \mathcal{D}_{|i\rangle}(u_s) + c_s^\varepsilon g(u_s) \right]$$

Let $|S_I| \equiv n_I$ denote the number of recorded samples for the i -th measurement operator. Then, for the feasible set $U = \{c_s^{(0)}, c_s^{(1)}, c_s^{\text{noise}} \in \{0, 1\}, \mu_1, \mu_2, \Sigma_1, \Sigma_2, \alpha_1, \alpha_2\}$, \mathbb{IQP} corresponds to the following nonconvex problem:

$$\begin{aligned} \mathbb{IQP}_{\mathcal{D}_{|0\rangle,|1\rangle}}(u_s) &:= \arg \min_U f_{\mathbb{IQP}} \\ \text{s.t. } & \sum_{s=1}^{|S_I|} c_s^{(i)} = \alpha_i |S_I| \\ & 1 = \sum_{j=0}^2 \alpha_j. \end{aligned} \quad (11)$$

Notice that there is no need to perform the inversion for Σ_i^{-1} : one can optimize the matrix variable, whose meaning is to be the inverse of the covariance.

Refining the interpretation of (11) as a map from the IQ-plane data corresponding to the σ_I measurement observable to the space of b_I we have:

$$\begin{aligned} \mathbb{IQP}_I : (\Omega_{\sigma_I}; \mathcal{D}_{|0\rangle}, \mathcal{D}_{|1\rangle}) &\rightarrow [-1, 1], \\ u_s &\mapsto (b_I)_s. \end{aligned} \quad (12)$$

Both the bilevel problem (8) and its lower level problem (11) are not trivial. However, in some settings, significant progress can be made.

First, let us consider the simplest setting, where the parameters of Equation (52) are known and either there is no contamination ($\alpha_2 = 0$)

or the contaminated samples can be identified. When one considers this “noise-less” case, Problem (11) corresponds to the well-known problem of the degree of membership (posterior information) of the samples, whose simplest case is:

$$\beta_{|i\rangle}(u_s) = \arg \max_{i \in \{0,1\}} N \left\{ \mathbf{X}_i(u_s) \right\}, \quad (13)$$

with $\beta_{|i\rangle}$ relating to the b vector as prescribed in Equation (3), although the role of the index is different in this context: we fix $\beta_{|i\rangle} := (\beta_I)_{|i\rangle}$, for some I . Furthermore, N is a normalization factor that we set equal to one, and

$$\mathbf{X}_i(u_s) := -(u_s - \mu_i)^\top \Sigma_i^{-1} (u_s - \mu_i), \quad (14)$$

and the decision rule is to assign each sample u_s to the cluster whose mean minimizes the Mahalanobis distance. Prob. (13) has a solution that is computable in linear time. Note that by expanding the terms in (14), we can define a PSD matrix

$$\mathbf{F}_{|i\rangle}^{(u)} = \left(\mu_i^\top \Sigma_i^{-1} - \mu_i^\top \Sigma_i^{-1} \mu_i \right). \quad (15)$$

Then (13) can be written as:

$$\beta_{|i\rangle}(u_s) = \arg \max_{i \in \{0,1\}} \left(\tilde{u}_s^\top \mathbf{1} \right) \mathbf{F}_{|i\rangle}^{(u)} \tilde{u}_s, \quad (16)$$

where $\tilde{u}_s := (u_s^\top \otimes_{\text{Kron}} \mathbf{1})^\top$. Alternatively:

$$\gamma_{|i\rangle}(u_s) = \text{softmax}_i \left(u_s^\top \mathbf{1} \right) \mathbf{F}_{|i\rangle}^{(x)} \begin{pmatrix} u_s \\ 1 \end{pmatrix}, \quad (17)$$

where softmax is defined as

$$\text{softmax}_i(u_s) = \frac{\exp(y_i(u_s))}{\exp(y_0(u_s)) + \exp(y_1(u_s))}, \quad (18)$$

such that $\gamma_{|0\rangle}^{(u_s)} + \gamma_{|1\rangle}^{(u_s)} = 1$, where, by definition, $\gamma_{|i\rangle}(u_s)$ will be in the interval $[0, 1]$.

When $\mathbf{F}_{|i\rangle}$ are nonnegative, this yields a strongly convex, unconstrained lower-level problem, which in turn can be substituted by its first-order optimality conditions. Then, it is possible to formulate the SDP (8) with additional constraints, taking into account all measurement basis operators. Explicitly, we have:

$$\begin{aligned} \text{QST}_A := \arg \min_{b, \hat{\rho}, \gamma} & \quad \|\text{Avec}(\hat{\rho}) - b\|_2^2 & (19) \\ \text{subject to} & \quad \text{Tr}(\hat{\rho}) = 1 \\ & \quad \hat{\rho} \in \mathbb{S}_+^2 \\ & \quad b = (b_x \ b_y \ b_z)^\top \\ & \quad b_u = \gamma_{|0\rangle}^{(u_s)} - \gamma_{|1\rangle}^{(u_s)} \\ & \quad \gamma_{|i\rangle}^{(u)} = \sum_{u_s} \text{softmax}_i \tilde{u}_s^\top \mathbf{F}_{|i\rangle}^{(u)} \tilde{u}_s \end{aligned}$$

for all elements u_s . This bilevel SDP (19) can then be extended, for instance, toward the unknown parameters of the Gaussian mixture and adversarial noise.

When the mixture model is contaminated by noise, that is, $\alpha_2 > 0$, we need to consider a constrained optimization problem. When the mean vectors μ_i of Equation (52) are unknown but the covariance matrices Σ_i are known, the estimation of the mean vectors $\hat{\mu}_i$ and mixture weights \hat{a}_i in the lower-level problem (11) corresponds to a nonconvex, but commutative polynomial optimization problem. Although this makes the problem nontrivial, it has been studied [24]. Finally, when both the mean vector and the covariance matrices of Equation (52) are unknown and there is contamination ($\alpha_2 > 0$), the lower-level problem (11) then corresponds to a nonconvex noncommutative (i.e., operator-valued) polynomial optimization problem. One can again solve such a bilevel polynomial optimization problem with a nonconvex lower-level problem using hierarchies of semidefinite programming relaxations. All of these more complicated scenarios are discussed in the supplementary material.

4 A simple example

To illustrate the importance of solving the joint problem, rather than decomposing it into discrimination and quantum state estimation, let us consider an example in which a state is estimated using information from input-output data in the presence of normally distributed noise with unity covariance and mean $\mu_{\text{noise}} = (-3.5, -3.5)$. Table 1 shows that the estimates of the b -vector can have a substantial error as the number of noise samples increases. This, in turn, results in inaccurate state estimation using the decomposition. In contrast, the error in the reconstruction of the

density matrix using the bilevel approach (19) in the Frobenius norm (in the rightmost column) does not increase with the number of samples of noise as fast as in the decomposed approach. In particular, in a low-noise regime (where for each projection operator, there are up to 75 samples of noise admixed to 5,000 measurements), the bilevel approach seems very robust.

Noise	b	b_x	b_y	b_z	Error
0	Orig.	-0.0008	-0.4674	-0.902	0
0	Est.	-0.0011	-0.466	-0.898	0.0022
10	Est.	-0.0012	-0.4616	-0.892	0.0015
25	Est.	-0.0036	-0.4636	-0.8856	0.0051
50	Est.	-0.0032	-0.458	-0.892	0.0026
75	Est.	-0.004	-0.4634	-0.878	0.0088
100	Est.	-0.9952	-0.9864	-0.8864	0.5021
150	Est.	-0.998	-0.992	-0.8815	0.5043
250	Est.	0.9916	0.9852	-0.8816	0.5026
500	Est.	0.9948	-0.9892	-0.8784	0.5044
750	Est.	0.936	-0.992	-0.8828	0.4870
1000	Est.	-0.992	-0.9932	-0.8888	0.5005
1500	Est.	0.9948	0.994	0.8896	1.3222
2000	Est.	0.994	0.99	-0.8924	1.3226

Table 1: Error in the estimation of the b -vector as a function of the number of samples of Gaussian noise admixed to 5,000 measurements per projection operator: The first row denotes the original value of the b vector (Orig.) while the subsequent rows (Est.) present estimates thereof, with the estimates of the b -vector obtained using an EM algorithm displayed in columns b_x , b_y , and b_z . The error in the reconstruction of the density matrix using the bi-level approach (19) in Frobenius norm is displayed in the right-most column.

5 Extensions

One could apply a similar bilevel view to a number of related problems. For relevant work, in relation to polynomial optimization methods, see Ref. [25].

5.1 Quantum Hamiltonian Identification

The state of a quantum system, such as the superconducting qubit in which we are interested, evolves in time from the input Hilbert space \mathcal{H}_{in} to the output Hilbert space \mathcal{H}_{out} according to a quantum Hamiltonian operator $H : \mathcal{H}_{\text{in}} \rightarrow \mathcal{H}_{\text{out}}$ that satisfies the Liouville evolution equation:

$$\frac{d\rho(t)}{dt} = -\frac{i}{\hbar}[H, \rho(t)]. \quad (20)$$

When considering the discrete-time evolution of ρ_i at time $t = i$ to ρ_{i+1} at time $t = i + 1$, the discrete analog of Eq. (20) can be written as follows using the Kraus map (Kraus operator sum representation):

$$\rho_{i+1} = \mathcal{E}(\rho_i) \quad (21)$$

$$= \sum_{k=1}^{d^2-1} \mathbf{E}_k \rho_i \mathbf{E}_k^\dagger, \quad (22)$$

where $\sum_{k=1}^{d^2-1} \mathbf{E}_k^\dagger \mathbf{E}_k = \mathbf{1}$ and \mathcal{E} denote the unknown quantum operation responsible for the evolution of the density matrix. To perform quantum Hamiltonian identification (QHI), we sample the unknown process m times, resulting in output state trajectories indexed by the lower index (see below). We introduce the following notation for the output and estimated density-matrix trajectories:

$$\begin{aligned} \rho_{\text{out}}^{(j)}(t = i) &\equiv \rho_i^{(j)} \\ \rho_{\text{est}}^{(j)}(t = i) &\equiv \hat{\rho}_i^{(j)} \end{aligned} \quad (23)$$

where trajectory $j \in \{1, \dots, N\}$. The index i here denotes the ordinal number of the sample (discrete time). We model the evolution of the states as a linear dynamical system:

$$\begin{aligned} \rho_i^{(j)} &= \mathbf{G} \rho_{i-1}^{(j)}, \\ \hat{\rho}_i^{(j)} &= \mathbf{J} \rho_i^{(j)}. \end{aligned} \quad (24)$$

Here \mathbf{G}, \mathbf{J} are the system matrices that we are interested in recovering. Effectively, \mathbf{G} corresponds to the evolution matrix (Hamiltonian), while \mathbf{J} is a matrix that transforms the hidden state to the observed state measured by the apparatus. To this end, we define the loss function:

$$f_{\text{loss}} = \sum_{i,j} \left\| \rho_i^{(j)} - \hat{\rho}_i^{(j)} \right\|_F^2 \quad (25)$$

Using the Kraus operator sum representation with fixed basis $\{\mathbf{E}_k\}_{k=1}^{d^2-1}$ in the space of Hermitian matrices \mathbb{H}_1^N , a first physical formulation of the state estimation problem, in terms of an SDP, takes the following form:

$$\begin{aligned} \min_U \quad & f_{\text{loss}}, \\ \text{s.t.} \quad & \rho_{i+1} = \sum_{k=1}^{d^2-1} \mathbf{E}_k \rho_i \mathbf{E}_k^\dagger \\ & \sum_{k=1}^{d^2-1} \mathbf{E}_k^\dagger \mathbf{E}_k = \mathbf{1}, \end{aligned} \quad (26)$$

where $\mathbf{U} = \{\boldsymbol{\rho}_i^{(j)}, \mathbf{E}_k\}$. By algebraic manipulations one can show that $\sum_{k=1}^{d^2-1} \mathbf{E}_k^* \mathbf{E}_k = \mathbf{G}$ and, as a result, Prob. (26) is reformulated as:

$$\begin{aligned}
& \min_S f_{\text{loss}}, \\
& \text{s.t. } \rho_i^{(j)} = \mathbf{G} \rho_{i-1}^{(j)}, \\
& \quad b_i^{(j)} = \mathbf{J} \rho_i^{(j)}, \\
& \quad \hat{\rho}_i^{(j)} = \text{QST}(b_i^{(j)}), \\
& \quad \rho_i^{(j)}, \hat{\rho}_i^{(j)} \in \mathbb{S}_+^2 \text{ for each } i, j \\
& \quad \text{Tr} \rho_i^{(j)} = \text{Tr} \hat{\rho}_i^{(j)} = 1.
\end{aligned} \tag{27}$$

Note that the index $i \in \{1, \dots, N\}$ in b_i corresponds to discrete time and should not be confused with $I \in \{x, y, z\}$. Therefore, we show that QHI can also be expressed as a bilevel SDP where the lower-level problem is Problem (8), the main object of study in this article.

6 Conclusions

We have considered, for the first time, a joint problem of quantum state tomography and discriminating between the states of a quantum system using the signal actually obtained in the dispersive readout, or similar mechanisms. This allows for lower sample complexity of quantum state tomography compared to traditional approaches, which discriminate first and perform state estimation second, while achieving the same error in the estimate of the state. Considering robust statistics [26] in this context allows many important extensions.

Acknowledgments

We wish to acknowledge Denys Bondar, Zakhar Popovych as well as Christos Aravanis for helpful discussions. Our work has been supported by OP VVV project CZ.02.1.01/0.0/0.0/16_019/0000765 “Research Center for Informatics”.

References

[1] Ashley Montanaro. Quantum algorithms: an overview. *npj Quantum Information*, 2(1), Jan 2016.

[2] G Wendin. Quantum information processing with superconducting circuits: a review. *Reports on Progress in Physics*, 80(10):106001, Sep 2017.

[3] John Preskill. Quantum computing in the nisq era and beyond. *Quantum*, 2:79, Aug 2018.

[4] Frank Arute et al. Quantum supremacy using a programmable superconducting processor. *Nature*, 574(7779):505–510, 2019.

[5] Isaac L. Chuang Michael A. Nielsen. *Quantum Computation and Quantum Information: 10th Anniversary Edition*. Cambridge University Press, 10 anv edition, 2011.

[6] G. Mauro D’Ariano, Matteo G.A. Paris, and Massimiliano F. Sacchi. Quantum tomography. In *Advances in Imaging and Electron Physics*, pages 205–308. Elsevier, 2003.

[7] Marcus Cramer, Martin B. Plenio, Steven T. Flammia, Rolando Somma, David Gross, Stephen D. Bartlett, Olivier Landon-Cardinal, David Poulin, and Yi-Kai Liu. Efficient quantum state tomography. *Nature Communications*, 1(1), December 2010.

[8] Yihui Quek, Stanislav Fort, and Hui Khoon Ng. Adaptive quantum state tomography with neural networks. *npj Quantum Information*, 7(1):105, 2021.

[9] Violeta N. Ivanova-Rohling, Niklas Rohling, and Guido Burkard. Optimal quantum state tomography with noisy gates, 2022.

[10] Hsin-Yuan Huang, Richard Kueng, and John Preskill. Predicting many properties of a quantum system from very few measurements. *Nature Physics*, 16(10):1050–1057, jun 2020.

[11] Göran Wendin. Quantum information processing with superconducting circuits: a review. *Reports on Progress in Physics*, 80(10):106001, 2017.

[12] T. Walter, P. Kurpiers, S. Gasparinetti, P. Magnard, A. Potočnik, Y. Salathé, M. Pechal, M. Mondal, M. Oppliger, C. Eichler, and A. Wallraff. Rapid high-fidelity single-shot dispersive readout of superconducting qubits. *Phys. Rev. Applied*, 7:054020, May 2017.

- [13] S Schaal, I Ahmed, JA Haigh, L Hutin, B Bertrand, S Barraud, M Vinet, C-M Lee, N Stelmashenko, JWA Robinson, et al. Fast gate-based readout of silicon quantum dots using josephson parametric amplification. *Physical review letters*, 124(6):067701, 2020.
- [14] D. T. McClure, Hanhee Paik, L. S. Bishop, M. Steffen, Jerry M. Chow, and Jay M. Gambetta. Rapid driven reset of a qubit readout resonator. *Phys. Rev. Applied*, 5:011001, Jan 2016.
- [15] Jeongwan Haah, Aram W. Harrow, Zhengfeng Ji, Xiaodi Wu, and Nengkun Yu. Sample-optimal tomography of quantum states. In *Proceedings of the Forty-Eighth Annual ACM Symposium on Theory of Computing*, STOC '16, page 913–925, New York, NY, USA, 2016. Association for Computing Machinery.
- [16] Peng Duan, Zi-Feng Chen, Qi Zhou, Wei-Cheng Kong, Hai-Feng Zhang, and Guo-Ping Guo. Mitigating crosstalk-induced qubit readout error with shallow-neural-network discrimination. *Phys. Rev. Applied*, 16:024063, Aug 2021.
- [17] JL O'Brien, GJ Pryde, AG White, TC Ralph, and D Branning. Demonstration of an all-optical quantum controlled-not gate. *Nature*, 426:264 – 267, November 2003.
- [18] Jens Koch, Terri M. Yu, Jay Gambetta, A. A. Houck, D. I. Schuster, J. Majer, Alexandre Blais, M. H. Devoret, S. M. Girvin, and R. J. Schoelkopf. Charge-insensitive qubit design derived from the cooper pair box. *Physical Review A*, 76(4), Oct 2007.
- [19] Evan Jeffrey, Daniel Sank, J. Y. Mutus, T. C. White, J. Kelly, R. Barends, Y. Chen, Z. Chen, B. Chiaro, A. Dunsworth, A. Megrant, P. J. J. O'Malley, C. Neill, P. Roushan, A. Vainsencher, J. Wenner, A. N. Cleland, and John M. Martinis. Fast accurate state measurement with superconducting qubits. *Phys. Rev. Lett.*, 112:190504, May 2014.
- [20] Thomas Alexander, Naoki Kanazawa, Daniel J Egger, Lauren Capelluto, Christopher J Wood, Ali Javadi-Abhari, and David C McKay. Qiskit pulse: programming quantum computers through the cloud with pulses. *Quantum Science and Technology*, 5(4):044006, 2020.
- [21] Jeroen P. G. van Dijk, Edoardo Charbon, and Fabio Sebastiano. The electronic interface for quantum processors, 2019.
- [22] W. H. Zurek. Pointer Basis of Quantum Apparatus: Into What Mixture Does the Wave Packet Collapse? *Phys. Rev. D*, 24:1516–1525, 1981.
- [23] Henry Wolkowicz, Romesh Saigal, and Lieven Vandenbergh. *Handbook of semidefinite programming: theory, algorithms, and applications*, volume 27. Springer Science & Business Media, 2012.
- [24] V. Jeyakumar, J. B. Lasserre, G. Li, and T. S. Pham. Convergent semidefinite programming relaxations for global bilevel polynomial optimization problems. *SIAM Journal on Optimization*, 26(1):753–780, 2016.
- [25] Denys I. Bondar, Zakhar Popovych, Kurt Jacobs, Georgios Korpas, and Jakub Marecek. Recovering models of open quantum systems from data via polynomial optimization: Towards globally convergent quantum system identification, 2022.
- [26] Peter J Huber. *Robust statistics*, volume 523. John Wiley & Sons, 2004.
- [27] E. de Klerk. *Aspects of semidefinite programming: Interior point algorithms and selected applications*. Number 65 in Applied optimization, ISSN 1384-6485. Kluwer Academic Publishers, Netherlands, 2002. Pagination: xvi, 283.
- [28] S. Dempe and J. Dutta. Is bilevel programming a special case of a mathematical program with complementarity constraints? *Mathematical Programming*, 131(1-2):37–48, 2010.
- [29] J. Frederic Bonnans and Alexander Shapiro. Optimization Problems with perturbations : A Guided Tour. Research Report RR-2872, INRIA, 1996. Projet PROMATH.
- [30] Miguel Navascués, Stefano Pironio, and Antonio Acín. A convergent hierarchy of semidefinite programs characterizing the set of quantum correlations. *New Journal of Physics*, 10(7):073013, Jul 2008.

- [31] Jiawang Nie, Li Wang, Jane Ye, and Suhan Zhong. A lagrange multiplier expression method for bilevel polynomial optimization. *arXiv preprint arXiv:2007.07933*, 2020.
- [32] Stephan Dempe, Floriane Mefo Kue, and Patrick Mehlitz. Optimality conditions for special semidefinite bilevel optimization problems. *SIAM Journal on Optimization*, 28(2):1564–1587, 2018.
- [33] Chi Jin, Yuchen Zhang, Sivaraman Balakrishnan, Martin J Wainwright, and Michael I Jordan. Local maxima in the likelihood of gaussian mixture models: Structural results and algorithmic consequences. In D. Lee, M. Sugiyama, U. Luxburg, I. Guyon, and R. Garnett, editors, *Advances in Neural Information Processing Systems*, volume 29. Curran Associates, Inc., 2016.
- [34] Naum Z Shor. Quadratic optimization problems. *Soviet Journal of Computer and Systems Sciences*, 25:1–11, 1987.
- [35] Naum Zuselevich Shor. Dual quadratic estimates in polynomial and boolean programming. *Annals of Operations Research*, 25(1):163–168, 1990.
- [36] Michael Grant and Stephen Boyd. CVX: Matlab software for disciplined convex programming, version 2.1. <http://cvxr.com/cvx>, March 2014.
- [37] R. Gupta and Yihua Chen. Theory and use of the em algorithm.

For the convenience of the reader, we provide additional background material on mathematical optimization and the dispersive readout, as well as further numerical illustrations in the supplementary material.

A Further background on mathematical optimization

A.1 Semidefinite Programming

Semidefinite programming corresponds to optimization problems where the objective function is a linear function that involves a positive semidefinite matrix and constraints are given as an intersection of the convex cone of positive semidefinite matrices and an affine subspace [27]. Let us recall the most basic definitions: Consider a matrix $X \in \mathbb{S}^n$, that is a $n \times n$ symmetric matrix and let $C(X)$ a linear function of X :

$$C(X) = \langle C, X \rangle \quad (28)$$

$$= \text{Tr}(C^\top X) \quad (29)$$

$$= \sum_{i=1}^n \sum_{j=1}^n C_{ij} X_{ij}. \quad (30)$$

Definition 1 A primal SDP is a convex optimization problem with data consisting of a symmetric matrix C and m symmetric matrices A_1, \dots, A_m , as well as the m -dimensional vector b . One looks for a feasible solution X . The optimum is denoted as p^* . The problem takes the form:

$$\begin{aligned} & \text{minimize} && \langle C, X \rangle \\ & \text{such that} && \langle A_i, X \rangle = b_i, \\ & && X \succeq 0. \end{aligned} \quad (31)$$

Definition 2 The dual SDP to the primal SDP (31) is a convex optimization problem with data consisting of the same symmetric matrix C , same m symmetric matrices A_1, \dots, A_m , same m -dimensional vector b as well as an m -dimensional vector y and a matrix S . One seeks a feasible solution (y, S) and the optimum is denoted as d^* . The problem takes the form:

$$\begin{aligned} & \text{minimize} && \sum_{i=1}^m y_i b_i \\ & \text{such that} && \sum_{i=1}^m y_i A_i + S = C, \\ & && S \succeq 0. \end{aligned} \quad (32)$$

Definition 3 If feasible solutions X for the primal SDP and (y, S) for the dual SDP exist, then the duality gap is defined as:

$$\langle C, X \rangle - \sum_{i=1}^m y_i b_i \geq 0. \quad (33)$$

A.2 The standard SDP formulation of QST

The shape-constrained least-squares (introduced in the main article)

$$\|\mathbf{Avec}(\hat{\rho}) - b\|_2^2, \quad (34)$$

can be solved using first-order algorithms. Nevertheless, in this article, we will reformulate it as a semidefinite programming (SDP) problem [23]:

$$\begin{aligned} \text{QST}_{\mathbf{A}}(b) &:= \arg \min_{\hat{\rho} \succeq 0} \|\mathbf{Avec}(\hat{\rho}) - b\|_2^2 \\ &\text{subject to} \quad \text{Tr}(\hat{\rho}) = 1 \\ &\quad \hat{\rho} \in \mathbb{S}_+^2, \end{aligned} \quad (35)$$

where \mathbb{S}_+^n denotes the space of complex-valued positive-semidefinite symmetric matrices. Note this is precisely the same as Eq. (7). Solving the SDP (35) can be seen as a map from the space of recorded measurements b to the space of estimates $\hat{\rho}$, as suggested in Equation (4) in the main body. Prob. (35) easily generalizes to (i) other measurement-basis choices as well as to (ii) higher-level systems by the corresponding generalization of \mathbf{A} and b . The convexity is preserved, as the subspace of all density matrices embedded in the space of all Hermitian operators that act on a Hilbert space \mathcal{H} forms a convex subspace.

Evaluation map

In Prob. (7), we show how to construct the matrix \mathbf{A} for any measurement basis, but we have to assume that b is given. Generically, the b vector can be seen as a function from the space of the possible quantum-device measurements $\Omega_{\mathbf{M}}$ for the observable \mathbf{M} to the interval of empirical estimates $B := [-1, 1]$. Let us denote by $\Omega_{\mathbf{M}}^B$ the set of all maps $f_j : \Omega_{\mathbf{M}} \rightarrow B$, parametrized by $j \in \mathbb{Z}$. Then $b_I := \text{ev}(f_j, \{s_1, \dots, s_{n_I}\})$, where $\{s_1, \dots, s_{n_I}\} \in \Omega_{\mathbf{M}}$ and ev is the evaluation map. In the following subsection, we will pick an element of $\Omega_{\mathbf{M}}^B$, for $\mathbf{M} \in \{\sigma_x, \sigma_y, \sigma_z\}$, that allows us to re-formulate Problem (7) as a bilevel problem, i.e., an optimization problem that involves at

least one constraint to the optimizers of another well-defined optimization problem.

A.3 Bi-level optimization

Following [28] a bilevel optimization problem can be considered as the following optimization problem:

$$\begin{aligned} & \text{minimize} && F(x, y) \\ & \text{such that} && G(x) \leq 0 \\ & && y \in \arg \min_y f(x, y) \\ & && \text{subject to } g(x, y) \succeq 0 \end{aligned} \quad (36)$$

Here, $F, f : \mathbb{R}^n \times \mathbb{R}^m \rightarrow \mathbb{R}$, also $G : \mathbb{R}^n \rightarrow \mathbb{R}^k$ and $g \in \mathbb{S}_+^p$, the space of $p \times p$ PSD matrices. Problem (36) is an optimization problem called the upper-level whose constraint region is determined implicitly by the graph of the solution set mapping of another mathematical optimization problem, the lower-level problem which is defined as

$$\begin{aligned} & \text{minimize} && f(x, y) \\ & \text{subject to} && \text{subject to } g(x, y) \succeq 0 \end{aligned} \quad (37)$$

For $x \in \mathbb{R}^m$, $y \in \mathbb{R}^n$ and $\Omega \in \mathbb{S}^p$, the space of $p \times p$ symmetric matrices, one can introduce the Lagrangian:

$$L(x, y, \Omega) := f(x, y) + \langle \Omega, g(x, y) \rangle \quad (38)$$

and recall that the lower-level feasible set is $Y = \{y \in \mathbb{R}^n | g(x, y) \in \mathbb{S}_+^p\}$ and solution set mapping $\Psi(x) = \arg \min_y \{f(x, y) | y \in Y(x)\}$. The set of regular Lagrange multiplier matrices of (36) is defined as:

$$\begin{aligned} \Lambda(x, y) := \{ \Omega \in \mathbb{S}^p | 0 = \nabla_y L = \langle \Omega, g \rangle \\ \text{such that } g \in \mathbb{S}_+^p, \Omega \in \mathbb{S}_-^p \}. \end{aligned} \quad (39)$$

Assumption 1 *The functions F and G are continuously differentiable, while f and g are twice continuously differentiable. For any $x \in Q$, where $Q = \{x \in \mathbb{R}^n | G(x, y) \leq 0\}$, the map $y \mapsto f(x, y)$ is convex, whereas the map $y \mapsto g(x, y)$ is \mathbb{S}_-^p -convex. Moreover, we assume*

$$0 = \nabla_y \langle \Omega, g(x, y) \rangle, \quad (40)$$

$$0 = \langle \Omega, g(x, y) \rangle, \quad (41)$$

$$\Omega \in \mathbb{S}_-^p \iff \Omega = 0. \quad (42)$$

$$(43)$$

Using [29, Prop. 3.2], we see that

$$\forall (x, y) \in Q \times \mathbb{R}^m, \quad y \in \Psi \iff \Lambda(x, y) \neq \emptyset. \quad (44)$$

Here, $\Psi : \mathbb{R}^n \rightarrow \mathbb{R}^m$ is the solution map of the lower-level problem:

$$\Psi := \{f(x, y) | g(x, y) \in \mathbb{S}_+^p\}. \quad (45)$$

Moreover, for any $(x, y) \in \text{gph} \Psi \cap (Q \times \mathbb{R}^m)$ the set $\Lambda(x, y)$ is non-empty, convex, and compact. This justifies the substitution of the lower-level problem with the KKT conditions into Prob. (36):

$$\begin{aligned} & \min_{x, y, \Omega} && F(x, y) \\ & \text{such that} && G(x, y) \leq 0 \\ & && \nabla_y L = 0 \\ & && g(x, y) \succeq 0 \\ & && \Omega \in \mathbb{S}_-^p \\ & && \langle \Omega, g(x, y) \rangle = 0. \end{aligned} \quad (46)$$

In [28], the authors show that a classical bi-level programming problem and its KKT reformulation are equivalent with respect to global optimal solutions, whereas these problems do not need to coincide with respect to local optima.

B Further background on the dispersive readout

In this section, we provide further details on the dispersive readout and the IQ-plane. We want to remind the reader that the notion of discrimination refers to the process of determining whether the qubit was measured in the $|0\rangle$ or the $|1\rangle$ eigenstate with respect to the measurement operator \mathcal{M} as discussed in Sec. 1. In the dispersive readout, the readout chain is composed of the three levels of output data: level 0 *raw data*, level 1 *I-Q plane data* and level 2 *discriminated data*. The output response pulse (at level 0) can be mapped to a complex number (at level 1) that can be decomposed as the amplitude response I and the phase response Q and its precise meaning is explained below. Repetition of the measurement n times yields a mixture of two distributions, as shown in Figure 4.

As described in Sec. 2, the measurement process in a device such as the transmon qubit consists of probing the resonator with a pulse of frequency ω_{probe} . The maximum fidelity is achieved

when $\omega_{\text{probe}} = (\omega_C + \omega_C^X)/2$. A short readout pulse $s_{\text{r.o.}}(t)$ is then directed towards the resonator to interact with it, and thus interact with the qubit and be transmitted back to the control line. Assuming a linear pulse, its readout waveform reads:

$$s_{\text{r.o.}}(t) = A_{\text{r.o.}} \left(\cos(\omega_{\text{r.o.}} t) + \vartheta_{\text{r.o.}} \right), \quad (47)$$

where $A_{\text{r.o.}}$ is the amplitude of the probe pulse and $\vartheta_{\text{r.o.}}$ is the phase, both of which depend on the state of the qubit. We can rewrite the waveform as

$$s_{\text{r.o.}}(t) = \text{Re} \left(A e^{i(\omega_{\text{r.o.}} t + \vartheta)} \right) \quad (48)$$

$$= \text{Re} \left(A e^{i\theta} e^{i\omega_{\text{r.o.}} t} \right) \quad (49)$$

where we skipped the labels on the amplitude, frequency, and phase of the readout pulse. The quantity $s|_{\omega_{\text{r.o.}}} = A e^{i\theta}$ is called a phasor, and for a fixed frequency it completely specifies the pulse. The qubit resonance readout is performed by recording the *in-phase* component I and the *quadrature* component Q of the phasor:

$$s|_{\omega_{\text{r.o.}}} = A \left(\cos(\theta) + i \sin(\theta) \right) \quad (50)$$

$$= I + iQ, \quad (51)$$

i.e., Eq. (2). The I-Q plane $\simeq \mathbb{C}$ can be thought of as the phase space of the resonator-qubit coupled system. Once the signal has been transmitted back from the resonator to the control line, a comparison of the readout pulse to the original pulse is performed. Using the phase-shift between the known input pulse and the measured output, the qubit state can be mapped onto the complex I-Q plane.

Thus, a single pulse sent to the qubit maps to a point in the the complex I-Q plane. In total, N repetitions of the measurement provide a distribution that allows one to create a histogram of the recorded events and assign the probabilities of experiment outcomes. Repetition of the same procedure, with further copies of the state measured with different measurement operators of the n -dimensional measurement basis (albeit possibly with different pulse frequencies) allows one to study a n -dimensional histogram from which one can use to proceed to the estimation of the measured state.

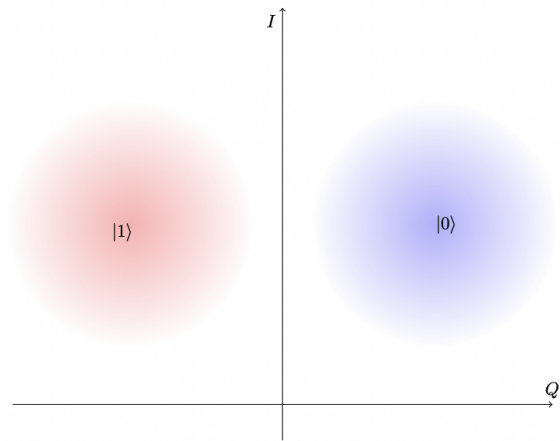


Figure 4: The I-Q plane data corresponds the phase space measurements of the response signal. While this figure is idealized, in reality, the scatter plot contains a lot of noise and robust techniques are required. Note that we can essentially identify the pointer basis $\{|g\rangle, |e\rangle\}$ to the standard qubit state basis $\{|0\rangle, |1\rangle\}$. The measurement described above has been performed in a fixed projective observable, say σ_z . The process needs to be repeated for the other two observables, σ_x, σ_y in order to get a full description of the state.

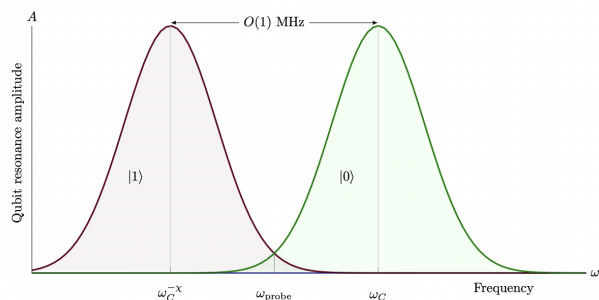


Figure 5: Resonance frequency-amplitude diagram for the qubit. The input probe pulse ω_{probe} excites the readout to either the green Lorentzian peak corresponding to $|0\rangle$ or the blue Lorentzian peak corresponding to $|1\rangle$. The sign of the phase difference of ω_{probe} to $\omega_{\text{r.o.}}$, the readout frequency, will reveal the pointer state the qubit is (with respect to one of the Pauli observables). The difference between the two resonance peaks is approximately 2χ and it is of the order of a few MHz.

C Details of our bilevel formulation

C.1 Known parameters and positive adversarial noise

When the mixture model is contaminated by noise, that is, $\alpha_2 > 0$, we need to consider a constrained optimization problem. This, in general, does not have a unique solution, and we need to consider the inclusion $b_I \in [\mathbb{I}\mathbb{Q}\mathbb{P}_{\mathcal{D}_{|0\rangle, |1\rangle}}(x)]_I$.

While in theory, one could consider the non-convex non-commutative polynomial optimization problem (10) from the main article, and consider the first-order optimality conditions of their (globally convergent) SDP relaxations [30, 31], a simpler approach is to consider a continuous relaxation in variables $U = \{f_s^{(0)}, f_s^{(1)}, f_s^{\text{noise}}\} \in [0, 1]$ over the polyhedron defined by Equation (10) from the main article. This convex optimization problem can be replaced by first-order optimality conditions under mild assumptions [31].

C.2 Unknown means and known covariance matrices

Let us recall Equation (9) from the main article:

$$f(u_s) = \sum_{i=\{1,2\}} \mathcal{D}_{|i\rangle}(u_s) + \alpha_2 g(u_s) \quad (52)$$

$$\text{where } \mathcal{D}_{|i\rangle}(u_s) := \frac{1}{\sqrt{2\pi}} \frac{\alpha_i}{|\Sigma_i|^{\frac{1}{2}}} e^{(u_s - \mu_i)^\top \Sigma_i^{-1} (u_s - \mu_i)},$$

Assume that the mean vectors μ_i of Eq. (52) are unknown, but the covariance matrices Σ_i are known. In this case, one has to estimate the mean vectors $\hat{\mu}_i$ as well as mixture weights \hat{a}_i the lower-level problem (10) from the main article corresponds to a nonconvex, but commutative POP. Although this makes the problem nontrivial, it has been studied [24]. Furthermore, the parameter space can be reduced by making the reasonable assumption $\mu_0^1 \approx -\mu_1^1, \mu_0^2 \approx \mu_1^2$, for $\mu_i = (\mu_i^1 \ \mu_i^2)^\top$. In particular, [24, Theorem 4.7] shows that assuming the Mangasarian-Fromovitz constraint qualification (or, less strictly, that there exists a representation of the feasible set of the lower-level problem as a finite union of closed convex sets with nonempty interiors), there exists an ϵ_0 , such that for all $\epsilon \in [0, \epsilon_0)$, one can obtain an ϵ -approximation of the problem by a convexification, which turns out to be an SDP that could be utilized, considering the recent study [32] of bilevel optimization with an SDP at the lower level.

The dimension of this SDP will grow rapidly with ϵ , but this is justified by the well-known issues [33] in estimating the parameters of a Gaussian mixture model using the EM algorithm, which would be the straightforward alternative. As a practically relevant alternative, one may consider the first available SDP within the hier-

archy, which resembles Shor's [34, 35] SDP relaxation and its KKT conditions.

C.3 Unknown means and unknown covariance matrices

Finally, let us assume that both the mean vectors and the covariance matrices of Equation (52) are unknown and there is contamination ($\alpha_2 > 0$). The lower-level problem (10) from the main article then corresponds to a nonconvex NCPOP. One can solve such a bilevel polynomial optimization problem with a nonconvex lower-level problem using hierarchies of semidefinite programming relaxations. Hierarchies of SDP relaxations of the NCPOP, such as the NPA hierarchy [30], essentially convert the original NCPOP to a series of SDP problems labeled by k such that for some k , the optimum of the SDP converges to the optimum of the NCPOP. Once the NCPOP is convexified in the form of an SDP, one can employ the KKT conditions in a manner similar to [24].

D Further numerical illustrations

In this section, we provide a numerical illustration of the method proposed in the main article.

Consider a two-level system in state:

$$\rho_{22} = \begin{bmatrix} 0.056 & i0.229 \\ i0.229 & 0.944 \end{bmatrix} \quad (53)$$

where we would like to estimate the eigenstate counts for the Pauli observables. Given a Gaussian mixture model for each $I \in \{x, y, z\}$ with mean vectors μ_0, μ_1 and covariance matrices Σ_0, Σ_1 , we can sample data that resemble the IQ-plane data using the state counts:

$$\begin{aligned} n_x^{(0)} &= 4996, & n_x^{(1)} &= 5004 \\ n_y^{(0)} &= 2663, & n_y^{(1)} &= 7337 \\ n_z^{(0)} &= 540, & n_z^{(1)} &= 9460. \end{aligned} \quad (54)$$

We consider two spherical Gaussians of means $\mu_0 = (2.5 \ 2.0)^\top$, $\mu_1 = (-2.5 \ 2.0)^\top$. We sample the first Gaussian with frequency $n_I^{(0)}/n_I$ and the second Gaussian with frequency $n_I^{(1)}/n_I$, $I \in \{x, y, z\}$. We perform $n = 10,000$ measurements of the state with respect to each of the

elements in the Pauli basis to obtain values for the empirical estimates of the expectation values of the Pauli observables:

$$b = \begin{bmatrix} -0.0006 & -0.4674 & -0.892 \end{bmatrix}^\top. \quad (55)$$

Traditionally, having the IQ-plane data, one would use EM algorithm for half of the dataset for calibration purposes, and then use the calibration results to decide the membership of the rest of the measured points. Using the counts (54) it is trivial to assign the estimates of the expectations of the measurement operators and to obtain the b vector:

$$b = \begin{bmatrix} -0.0044 & -0.4659 & -0.8979 \end{bmatrix}^\top. \quad (56)$$

which approximates the b -vector that one obtains from **Qutip** (55). Subsequently, the optimizer of the standard SDP formulation of QST, Equation (7) from the main article, is:

$$\rho_{(12)} = \begin{bmatrix} 0.0597 & -0.0008 + 0.2274i \\ -0.0008 - 0.2274i & 0.9403 \end{bmatrix}, \quad (57)$$

	$\hat{\mu}_0$	$\hat{\mu}_1$
σ_x	$(2.49752013 \ 1.98083953)^\top$	$(-2.50895142 \ 1.96288668)^\top$
σ_y	$(2.48478612 \ 1.99784236)^\top$	$(-2.55945933 \ 1.96636545)^\top$
σ_z	$(2.49009736 \ 1.99746892)^\top$	$(-2.60719554 \ 1.92029166)^\top$

Table 2: Mean vector estimates for each of the three spherical Gaussian mixture models using the EM algorithm.

	$\hat{\Sigma}_0$	$\hat{\Sigma}_1$
σ_x	$\begin{pmatrix} 0.9943854 & -0.0298129 \\ -0.0298129 & 0.987068 \end{pmatrix}$	$\begin{pmatrix} 0.9856472 & 0.009437 \\ 0.009437 & 0.9744658 \end{pmatrix}$
σ_y	$\begin{pmatrix} 1.0076411 & -0.0044255 \\ -0.0044255 & 0.994228 \end{pmatrix}$	$\begin{pmatrix} 0.9347116 & 0.0104711 \\ 0.0104711 & 0.9281853 \end{pmatrix}$
σ_z	$\begin{pmatrix} 1.0082151 & 0.0014959 \\ 0.0014959 & 0.9844126 \end{pmatrix}$	$\begin{pmatrix} 1.0102680 & -0.1381553 \\ -0.1381553 & 0.9478898 \end{pmatrix}$

Table 3: Covariance matrix estimates for each of the three spherical Gaussian mixture models using the EM algorithm.

	b_x	b_y	b_z
Qutip	-0.0006	-0.4674	-0.8920
ME	-0.0044	-0.4659	-0.8979
SDP	-0.0004	-0.4480	-0.8913

Table 4: Estimates for the b vector.

which, given the small supply of samples to the algorithm, is a good estimate of the true state (53). For comparison, using (55) we obtain a state estimate:

$$\rho_{\text{Qutip}} = \begin{bmatrix} 0.0571 & -0.0003 + 0.2321i \\ -0.0003 - 0.2321i & 0.9429 \end{bmatrix}. \quad (58)$$

Using our approach, Equation (8) from the main article, which utilizes the IQ-plane data directly, we explicitly count states using Equation (10) from the main article, to estimate the true state ρ (53) as:

$$\rho_{(24)} = \begin{bmatrix} 0.0544 & -0.0002 + 0.2240i \\ -0.0002 - 0.2240i & 0.9456 \end{bmatrix}. \quad (59)$$

The Frobenius norm of the difference, as computed by MATLAB[®], is $\|\rho_{\text{Qutip}} - \rho_{(12)}\|_F = 0.6455$ and $\|\rho_{\text{Qutip}} - \rho_{(24)}\|_F = 0.6406$, respectively, suggesting a modest improvement in the estimate of the quantum state. This numerical illustration provides only an anecdotal evidence of the improvement that can be obtained by considering the bilevel problem. We envision that further work could corroborate the observation on real data.

Both the standard approach to quantum state tomography as well as our approach, Equations (7) and (8) from the main body, can be written in MATLAB[®] using the CVX convex optimization library [36] in the SDP mode where the algorithm, in both cases, runs very fast. The state estimation \mathbf{X}_{12} requires knowledge of the b vector. This is achieved with the EM algorithm (see [37] for example) used on the training data obtained by sampling the Gaussians. On the other hand, the SPD that estimates \mathbf{X}_{24} , computes the b vector as part of the problem.

In Tables 2-4, we present the ME-estimations for the mean vectors and the covariance matrices for the three sets of Gaussian mixtures, as well as the values of the b vectors for the three different approaches.